Chem. Senses 37: 655–668, 2012

doi:10.1093/chemse/bjs048
Advance Access publication April 6, 2012

Tissue-Specific Effects of Allergic Rhinitis in Mouse Nasal Epithelia

Virginia McMillan Carr, Alan M. Robinson and Robert C. Kern

Department of Otolaryngology, Head and Neck Surgery, Feinberg School of Medicine, Northwestern University, Chicago, IL 60611, USA

Correspondence to be sent to: Virginia McMillan Carr, Department of Otolaryngology, Head and Neck Surgery, Feinberg School of Medicine, Northwestern University, Room 12-569, Searle Building, 303 E. Chicago Avenue, Chicago, IL 60611, USA.
e-mail: v-carr@northwestern.edu

Accepted March 1, 2012

Abstract

Allergic rhinitis (AR) can cause significant olfactory loss, but few studies have specifically investigated AR effects on olfactory and nasal respiratory tissues per se. To address this, we used a murine AR protocol employing nasal allergen infusion for both sensitization and challenges. Seven- to 11-week BALB/c mice were bilaterally infused with 1% ovalbumin (OVA) in phosphate-buffered saline (PBS) or PBS alone for 6 or 11 weeks, given single bilateral PBS or OVA infusions 24 h before sacrifice, or left untreated. High OVA-specific IgE serum levels and eosinophil infiltration confirmed AR induction. Olfactory (OE) and respiratory (RE) epithelia showed distinctly different responses, most conspicuously, massive eosinophil infiltration of immediately RE-subjacent *lamina propria*. In OE, such infiltration was minimal. Significant RE hypertrophy and hyperplasia also occurred, although OE organization was generally maintained and extensive disruption localized despite a 20% reduction in sensory neurons and globose basal cells after 11 weeks OVA. Pronounced Bowman's gland hypertrophy crowded both OE and olfactory nerve bundles. Cellular proliferation was widely distributed in RE but in OE was localized to normally thinner OE and RE-proximal OE, suggesting possible indirect RE influences. Terminal deoxynucleotide transferase (TdT) nick end labeling was greater in OE than RE and, in contrast to other effects, occurred with acute infusions and chronic PBS alone, often unilaterally. Following chronic OVA, AR-related bilateral increases appeared superimposed on those. These findings indicate AR effects on olfactory function may be complex, reflecting various levels of RE/OE responses and interactions.

Key words: allergic rhinitis, Bowman's glands, eosinophil infiltration, olfactory epithelium, respiratory epithelium

Introduction

Allergic rhinitis (AR) is the most common atopic disease (McCusker et al. 2002) and often leads to significantly reduced olfactory capabilities (Baroody and Naclerio 1991; Apter et al. 1995). To begin to examine AR effects on olfaction in a model system, we adapted the murine in situ nasal sensitization and challenge AR protocol of McCusker et al. (2002) and examined consequent nasal epithelial changes. The protocol involves intranasal delivery of small amounts of allergen for both sensitization and challenges, the rationale being that this more closely reflects natural human AR and asthma induction than do other murine models which rely on systemic sensitization (intraperitoneal or subcutaneous, with or without adjuvant) with only the subsequent challenges being nasal and often involving relatively large infusate volumes (e.g., Sato et al. 1999; Saito et al. 2001; Martin et al. 2005; Rahman et al. 2006; Ozaki et al. 2010). The use of a nonmicrobially derived allergen (ovalbumin, OVA) also avoids possible complications arising from use of microbial allergens, which may evoke additional innate, non-AR immune responses to specific microbe-associated molecular patterns (e.g., van de Rijn et al. 1998; Okano et al. 1999; Epstein et al. 2008). Using their protocol, McCusker et al. showed elevation of serum allergen-specific IgE and IgG levels, pronounced upper and lower airway eosinophil infiltration, and increased IL-5 and polymorphonuclear leukocyte presence in postchallenge bronchoalveolar lavage fluid, all indicators of AR. A more detailed histological analysis, however, was not carried out, especially with regard to olfactory (OE) and respiratory (RE) epithelia.

We have now undertaken such an analysis and have also included an additional longer period of allergen challenge, as

might occur with chronic or perennial allergen exposure. We find distinct RE and OE histological changes, RE-specific eosinophil *lamina propria* infiltration, and possibly enhanced OE changes in areas of closer than more distant RE proximity. Such findings suggest that nasal AR responses involve RE/OE and immune system interactions and that AR-related olfactory functional changes likely reflect events at multiple levels.

Materials and methods

Animals

Virus-free 7–11-week-old BALB/c mice (Charles River) were housed under conventional conditions in the Northwestern University animal facility. BALB/c mice were used because this strain had been found in studies using the *Schistosoma mansoni* egg antigen as the allergen to give more robust AR responses than either C57BL/6 or CBA/J mice (Okano et al. 1999). All procedures were carried out in accordance with the National Institutes of Health "Guide for the Care and Use of Laboratory Animals" and Northwestern IUCAC.

Mice were subjected to bilateral infusion of 7.5 μL of either filter-sterilized 1.0% ovalbumin (OVA; Grade V; Sigma) in phosphate-buffered saline pH 7.4 (PBS, prepared from a concentrate [OmniPur, EMD Chemicals]) or PBS alone. To maximize nasal cavity fluid dispersal, animals were gently held on their backs during infusion and maintained in that position until their efforts to expel the infusate ceased. Infusions followed the protocol in Figure 1a. Chronically exposed mice were treated for 6 or 11 weeks and sacrificed 1 day after the last infusion. Week 3 of the regimen was a rest period followed by single bilateral infusions on the Monday of Week 4. This third to fourth week break was found essential for maximizing immune responses at sacrifice in Week 6 (McCusker et al. 2002). In our extension of the McCusker et al. protocol to 11 weeks, we have included a similar break in Weeks 8–9. Acutely exposed mice received single bilateral OVA or PBS infusions followed by sacrifice 1 day later. Untreated control mice received neither OVA nor PBS prior to sacrifice. Two series of mice were processed, with a total of 50 animals overall (Figure 1b).

At the time of sacrifice, animals were deeply anesthetized with ketamine and xylazine (0.65 mg and 0.035 mg/g b.wt., respectively), blood collected by cardiac puncture, and the animals transcardially perfused with PBS followed by 4% paraformaldehyde in PBS. Following overnight postfixation at 4 °C in 4% paraformaldehyde, heads were trimmed, decalcified (Series I, 4 h, RDO [Apex Engineering]; Series II, 2 days, 2% Na citrate/4% formic acid), embedded in Paraplast (Oxford Labware), and sectioned coronally at 8 μm through the entire anterior–posterior extent of the nasal cavity. To examine nasal cell proliferation, Series II animals were injected with the thymidine analog 5-bromo-2′-deoxyuridine (BrdU; 0.05 mg/g b.wt. ip.; Sigma–Aldrich) 2 h prior to fixation.

Histology

For orientation and overall nasal histological examination of each animal, sections separated by 500–800 μm through the major extent of the OE-containing nasal cavity were mounted on slides and stained with hematoxylin and eosin (H&E). All subsequent histological procedures were carried out on serial sections sequentially ordered to these so that all processed sections from each locale were within 60–70 μm of each other. For each histological procedure, 8–10 sections were examined per animal, extending from the most anterior appearance of endoturbinate 2 (terminology of Liebeck 1975) to the fusion of endoturbinate 4 with the cribriform plate.

Both OE and RE cell counts were carried out in the above H&E serial sections in the anterior OE-containing region, from the initial appearance of endoturbinate 2 to the fusion of its dorsal and ventral arms. Three sections, separated by at least 500 μm, were examined for each animal. Counts of nuclear profiles were made along 100 μm strips at 100× magnification. For the OE, olfactory sensory neurons (OSNs), globose basal cells, and supporting cells were counted in 2–3 septal strips situated from 200 μm above the OE/RE transition zone to the top of the septum and in one strip along the facing OE of the dorsal arm of endoturbinate 2.

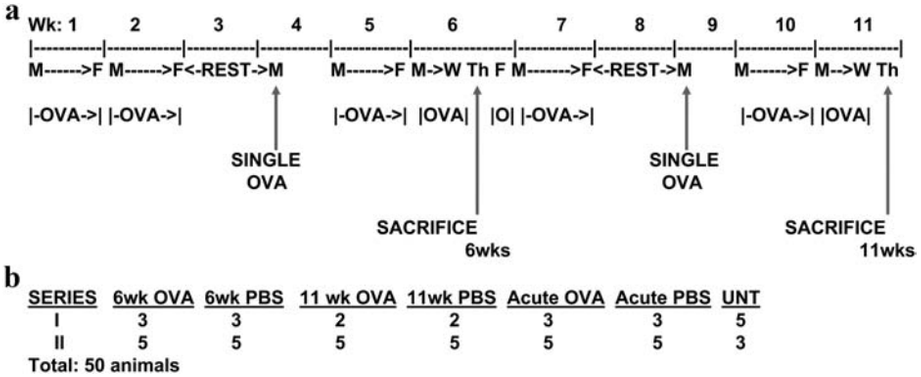

Figure 1 (**a**) Schedule for chronic nasal OVA infusions. The PBS infusion protocol was identical. (**b**) Distribution of mice used for each exposure schedule.

Septal strips were separated by at least 200 μm along the epithelial surface. In the RE, goblet and ciliated cells were counted in 2–3 strips along the septum and 1–2 strips along the RE of the facing nasal cavity wall, again situated at least 200 μm from OE/RE transition zones and separated by 200 μm. The OE counts were made in 11-week OVA-treated and untreated animals, the RE counts in 6-week OVA-treated and untreated animals, as explained in the Results. For both OE and RE, 6 OVA-treated animals and 4 untreated animals were examined, with totals of 17–23 strips for each epithelium per animal. Counts for each strip were made in triplicate and a mean calculated and tabulated. Overall means and standard errors were determined for each animal and for total values for each treatment.

The presence of eosinophils was visualized in one set of serial sections from each animal with the Luna stain (Luna 1968). Although the Luna stains erythrocytes as well as eosinophils, PBS exsanguination prior to fixation would have removed most erythrocytes. Distribution and hypertrophy of Bowman's glands in the OE-associated *lamina propria* were examined with Alcian blue pH 2.5 for acid mucopolysaccharides (http://library.med.utah.edu/WebPath/HISTHTML/MANUALS/ALCIAN.PDF) followed by H&E. Because of its OE association, Bowman's gland distribution provides a useful marker for the original location of any OE lost or replaced by RE.

Immunohistochemistry

Antibodies used were directed to BrdU (rabbit anti-BrdU, 1:1500, Abcam) and olfactory marker protein (OMP; goat anti-OMP, 1:4000, WAKO). Immunoreactivity was visualized by diaminobenzidine immunoperoxidase methodology using the appropriate Vector Elite ABC Kit with Fast Green FCF counterstaining. Antigen retrieval for BrdU immunoreactivity followed the manufacturer's directions: sections were heated in 2 N HCl 1 h at 37 °C followed by 12 min 0.1 M sodium tetraborate neutralization (pH 8.5). Sections of intestine from BrdU-injected animals served as positive controls.

Quantification of RE thickness

Measurements of RE thickness between the basement membrane and apical RE surface were made at 100× on the sections processed for anti-OMP immunohistochemistry from all Series I animals. OMP-stained sections were used to clearly distinguish between swollen RE and neighboring OE. Measurement sites in a given section were separated by at least 75 μm, giving an average of 150 measurements per animal.

TUNEL labeling for degenerating cells

Presence of degenerating cells was examined in Series II animals by terminal deoxynucleotide transferase (TdT) nick end labeling (TUNEL) procedures (ApopTag Plus Peroxidase Kit; Millipore). Three sections were processed per animal, selected to include anterior, mid, and posterior olfactory regions: regions showing, respectively, the anterior level of endoturbinate 2, the presence of all turbinates from ectoturbinate 2 through endoturbinate 3 or 4, and the region showing endoturbinate 4 just anterior to its fusion with the cribriform plate. Procedures followed manufacturer's directions except that Proteinase K was used at 7.5 μg/mL and TdT at 1% of the final reaction mixture. Omission of TdT controlled for the enzyme. Absence of staining in the olfactory bulb and other tissues and the expected increase in ipsilateral OE labeling in sections obtained from previous bulbectomy studies (Robinson et al. 2003) served as negative and positive controls, respectively. Because of recognized TUNEL variability, primary comparisons between treatment groups were made with slides processed simultaneously.

Imaging

Images were captured on a Leica DMRB microscope equipped with a Spot Insight Color Camera using the SPOT Basic software package (Diagnostic Instruments) and processed using Adobe Photoshop programs 6 and CS2. All image adjustments are noted in the appropriate captions.

OVA-specific IgE ELISAs

The blood samples collected at sacrifice were stored undisturbed at 4 °C overnight, centrifuged (14 000 rpm, 5 min), the sera collected and stored at –80 °C, and samples analyzed by enzyme-linked immunoabsorbant assay (ELISA) for OVA-specific IgE (Mouse OVA-IgE Kit; MD Biosciences).

Statistical analysis

Quantitative data were analyzed by the Mann–Whitney test using GraphPad Prism 4 software.

Results

Induction of AR

Allergen-specific IgE levels and strong eosinophil infiltration of nasal tissue, 2 major indicators of AR induction, were both greatly increased in the chronic OVA-exposed animals and in those alone.

OVA-specific IgE ELISA

Of the five 6-week OVA serum samples giving adequate analysis volume, 4 showed noticeably increased OVA-specific IgE levels; one showed none. Overall mean value for the 4 increased samples (185.6 ± 58.9 ng/mL, mean ± standard error of the mean) was highly significant compared with the 6-week PBS or untreated control values (both 0.0 ± 0.0 ng/mL) (Figure 2). All 11-week OVA samples analyzed showed large OVA-specific IgE increases and a highly significant mean increase over 11-week PBS values (5447.0 ± 2697.4 vs. 24.0 ± 24.0 ng/mL, respectively). The 11 week levels further divided

into 2 response groups, one high (10 434.0 ± 3387.7 ng/mL) and one lower (460.0 ± 181.2 ng/mL). Both represent significant increases ($P = 0.02$). Measured IgE level of each animal correlated with its subsequently analyzed histological features. Significantly, the single low-response 6-week OVA animal above was the only chronic OVA animal to show no eosinophil infiltration or histological change. That animal was used for comparative purposes only and omitted from further analysis.

No changes occurred in PBS- or acutely OVA-treated mice compared with untreated ones.

Eosinophil infiltration

Strong eosinophil infiltration occurred bilaterally in the nasal mucosa of all chronic OVA-treated animals except the single cited above (Figure 3). It did not occur in any other treatment group. Significantly, infiltration was strongly localized to the RE-associated *lamina propria*, predominantly immediately subjacent to the basement membrane but with some more deeply scattered cells as well (Figure 3a,b,f). In contrast, very few eosinophils occurred in sub-OE *lamina propria*, and most of those were scattered through the entire *lamina propria* rather than localized to the immediate OE-subjacent region (Figure 3a–e). The change from the RE- to the OE-associated pattern was striking and occurred within 200 μm of the RE/OE transition (Figure 3a). These OE/RE eosinophil distribution differences occurred uniformly throughout the entire nasal cavity. Few eosinophils occurred within the epithelia themselves (Figure 3b,f) or in nasal exudate (Figure 3b,d), suggesting possibly limited epithelial access.

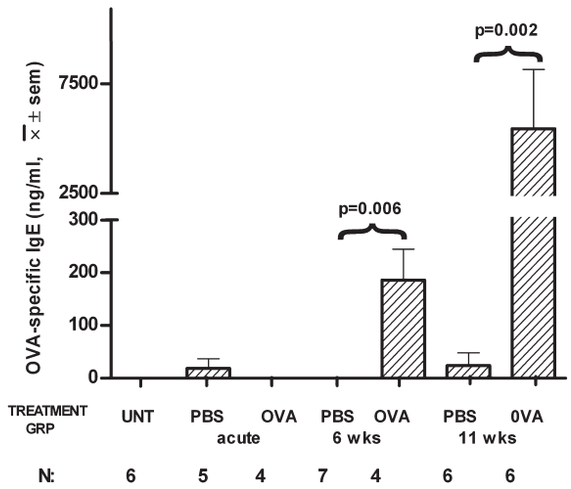

Figure 2 ELISA-determined mean cardiac blood serum levels of ovalbumin-specific IgE in mice treated with the various exposure protocols in Figure 1. UNT, untreated animals; PBS, 7.5 μL PBS bilateral nasal infusions; OVA, 7.5 μL 1.0% ovalbumin bilateral nasal infusions; *N* = number of serum samples analyzed.

Histological observations

Untreated, PBS-, and acutely OVA-exposed animals

All untreated animals showed histologically normal OE and RE (Figure 4). The OE was 60–80 μ thick and its 3 constituent cell layers readily identifiable. In the OE-subjacent *lamina propria*, Bowman's glands were unswollen and olfactory nerve bundles compactly filled with axons. Nasal RE was 8–15 μm thick, with ciliated, goblet, and basal cells clearly distinguishable. Other than slight RE thickening (below), PBS and acute OVA animals also showed normal nasal histologies.

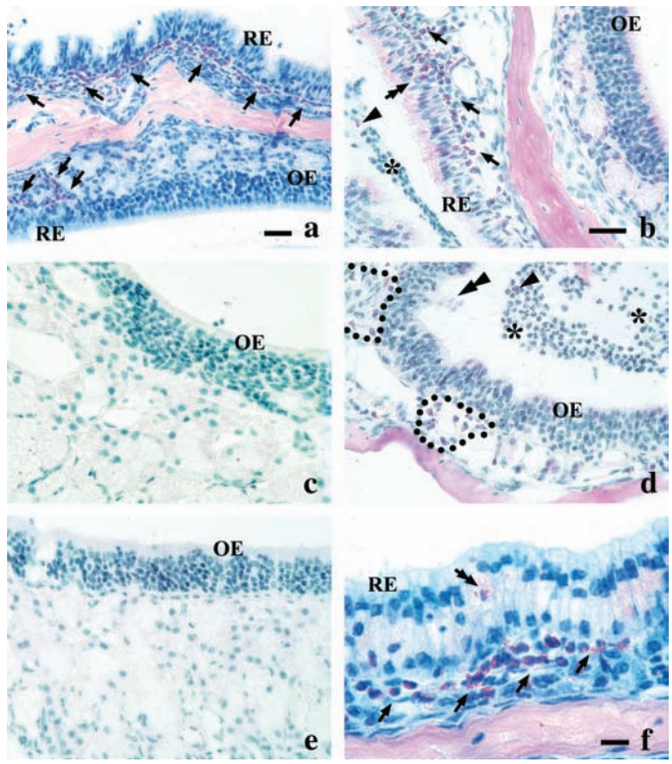

Figure 3 Luna procedure-stained eosinophils (red) in nasal tissues of animals exposed to OVA for 6 (**a**–**d**) and 11 weeks (**e**, **f**). Numerous eosinophils (e.g., arrows, a, b, f) occur in the *lamina propria* immediately subjacent to respiratory RE but are generally absent from the OE-subjacent *lamina propria* (a, b, c, e), even despite obvious OE disruption (c, e). The sharpness of the subepithelial eosinophil density decrease across the RE/OE transition is apparent in the lower surface of the turbinate shown in a. Nevertheless, occasional very disrupted OE regions do show subepithelial eosinophils but with a distribution across the entire *lamina propria* rather than as a concentrated layer in the immediate OE-adjacent area (dot-enclosed areas, d). Within the RE itself, eosinophils are rare (double arrows, b, f). Nasal exudate (asterisks, b, d) shows only occasional eosinophils (arrowheads). Shedding of multiple cells from the OE can be seen in d (double arrowhead). Brightness was enhanced in a and color adjusted in d to more readily show eosinophils. Calibration bars, a, b (for b–e), 25 μm; f, 10 μm.

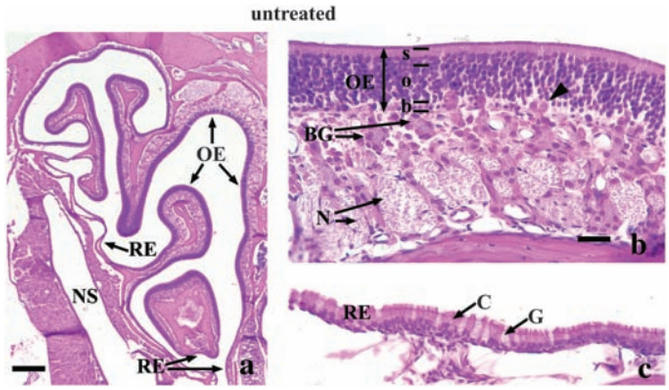

Figure 4 Hematoxylin and eosin stained sections through the nasal cavity of untreated control mice. (**a**) Low magnification of showing the distribution of olfactory (OE) and the thinner respiratory (RE) epithelia in the right nasal cavity of an untreated mouse. NS, lateral nasal sinus. (**b**, **c**) Higher magnifications of OE and RE, respectively, show their normal histologies. The OE basal, OSN, and supporting cell layers (b, o, s, respectively) are indicated. Double-headed arrow indicates OE thickness. Bowman's glands (BG) show no swelling or crowding of olfactory nerve bundles (N) in the *lamina propria* and the normal degree of protrusion into the OE (e.g., arrowhead). Olfactory nerve bundles show compact filling with olfactory neuron axons. In the RE, ciliated (C) and goblet cells (G) are distinct. Overall OE and RE appearances from chronic and acute PBS and acute OVA animals are similar. Image contrast and brightness have been adjusted over the entire figure. Calibration bars, a, 250 μm; b and c, 25 μm.

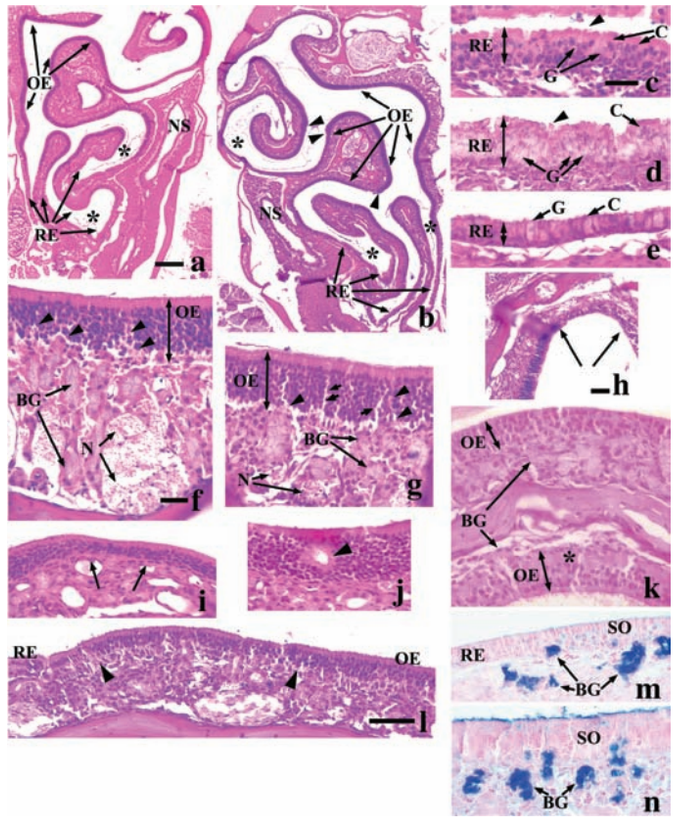

Figure 5 (**a**–**l**) Hematoxylin and eosin preparations from animals with 6 (a, c, f, h) and 11 weeks (b, d, g, i–l) chronic ovalbumin (OVA) exposure and 11 weeks PBS exposure (e). Abbreviations as in Figure 4. (a and b) Low magnifications from 6- (a) and 11-week (b) chronic OVA animals. RE swelling is apparent even at this magnification as is nasal exudate (asterisks) in the nasal cavity. Even at 11 weeks, OE changes are much less obvious (arrowheads, b). Nasal sinus epithelial swelling can also be seen. (c–e) Higher magnification through the RE of 6- and 11-week OVA- and 11-week PBS-exposed animals (c, d, e, respectively). Pronounced RE goblet cell swelling with surface crenelation occurs in chronic OVA animals. Surface blebbing is also apparent (arrowheads, c, d). At 6 weeks OVA exposure, goblet and ciliated cells can still be readily distinguished, but by 11 weeks, goblet cell hypertrophy makes this difficult. Slight RE hypertrophy relative to untreated control RE (Figure 4c) also occurs with chronic PBS treatment. (f–k) Higher magnifications through OE following chronic OVA exposure. (f, g) Most OE appears grossly normal at both chronic exposure periods. However, Bowman's glands are greatly swollen and appear to crowd olfactory nerve bundles in the *lamina propria*, especially by 11 weeks exposure (g). Disruptive BG protrusion into overlying OE also occurs (arrowheads, f, g). Nerve bundles appear much less densely packed than those of control animals (cf. Figure 4b). Small tears can also cross the OE (small arrows, g). (h–k) Small areas of OE also show more pronounced changes, including distinct thinning (h, i, between arrows) and presence of invaginated lacunae (arrowhead, j). Areas of cellular hypertrophy also occur, as seen in OE on a ventral, concave turbinate surface (asterisk) where OE is normally quite thin (k). (l) By 11 weeks OVA exposure OE disruption was often more noticeable in RE-proximal regions (center, between arrowheads) than more distally (to right). (**m**, **n**) Alcian blue-stained sections through the septal organ region (SO) of untreated control (m) and 11-week chronic OVA (n) animals. In chronic OVA animals, the SO itself completely disappears and is replaced by swollen RE, its original location indicated only by the presence of Alcian blue-stained Bowman's glands. Note, image sharpness was increased in k. Brightness and contrast were also adjusted over the entire figure. Calibration bars, a, 250 μm for a, b; c, 25 μm for c–e; f, 25 μm for f, g, i–n; h, l, 50 μm.

Chronic OVA- and PBS-exposed animals

RE. The most striking nasal changes following chronic OVA exposure occurred in the RE and consisted of pronounced RE swelling (Figure 5a–e). Swelling occurred uniformly throughout the RE at both 6 and 11 weeks exposure. Widespread associated surface crenelation also occurred. Mean RE thickness increases were highly significant relative to those in both chronic PBS-treated and untreated control animals (Figure 6a,b). As is typical in AR (e.g., Tesfaigzi et al. 2000; Rogers 2003; Locksley 2010), pronounced goblet cell swelling and hyperplasia (below) clearly contributed to this RE hypertrophy; and although RE cell identities were readily distinguishable at 6 weeks (Figure 5c), the swelling rendered them much less so at 11 weeks (Figure 5d). Confirming these observations, RE cell counts in 6-week OVA-treated mice showed highly significant increases in cell numbers (Figure 6c). Moreover, while the number of goblet and ciliated cells/100 μm increased 1.6-fold over untreated animals (59.5 ± 1.5 vs. 36.7 ± 1.0), the number of goblet cells alone increased 3.4-fold (24.2 ± 0.6 vs. 7.0 ± 0.3), and percentage of cells that were goblet cells increased 2.2-fold (42.4 ± 1.1 vs. 19.5 ± 0.8).

Unexpectedly, RE thickening also occurred with PBS and acute OVA treatments (Figure 6b). Increased thickness was not strikingly obvious on visual observation (Figure 5e); but all increases were highly significant, likely due to the large measurement numbers (200–450 per treatment group). Post-infusion time of onset of this non-AR-related swelling is not

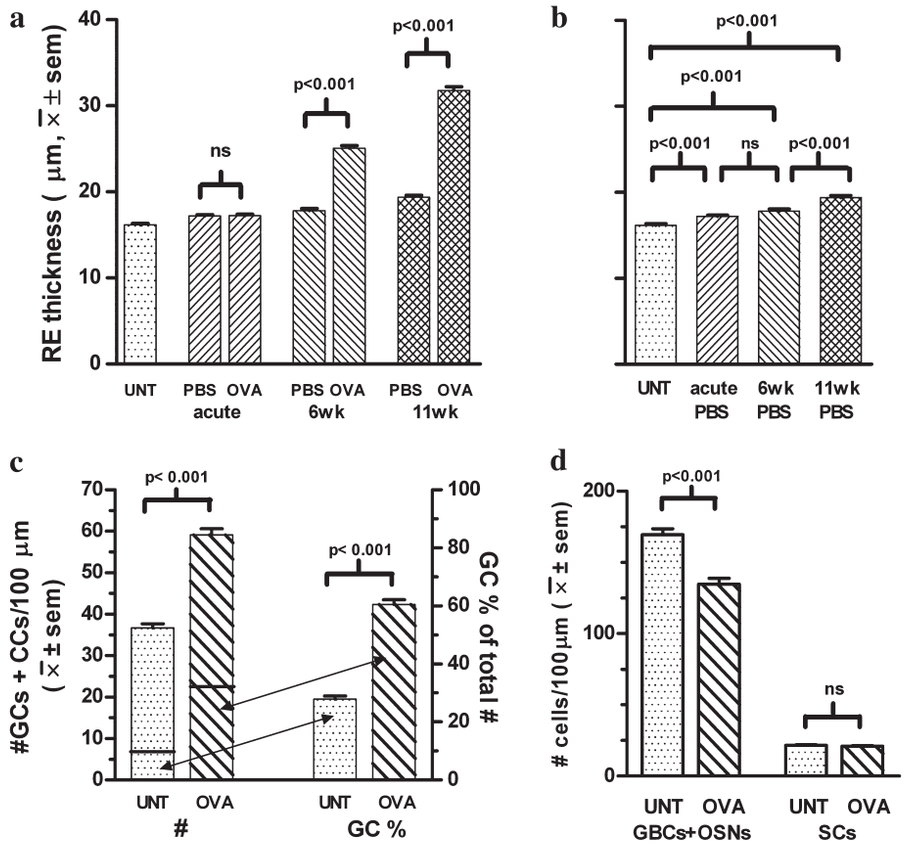

Figure 6 (**a**, **b**) Bar graphs showing mean RE thickness for untreated animals and for each PBS and OVA treatment regimen. (a) Comparisons of OVA and PBS values within each treatment period. (b) Comparisons of thicknesses from untreated and each set of PBS-treated animals. (**c**) Mean number of goblet cells (GCs) plus ciliated (CCs) cells per 100 μm in untreated RE and RE from 6-week OVA-treated animals (left *y*-axis) and the percentage of the counted cells that are goblet cells (right *y*-axis). Mean densities of goblet cells alone are indicated by lines across the respective bars on the left, with arrows connecting the respective densities and percentages. (**d**) Mean number of OE globose basal cells (GBCs) plus OSNs and of supporting cells (SCs) per 100 μm in untreated and 11-week OVA-treated mice. Details of counts and measurements are given in the text.

known, but the effect clearly persists through at least 24 h, the acute postinfusion survival period.

OE. In contrast to the uniform RE swelling, OVA-related OE changes were less obvious and more variable; and in most locales, OE appeared grossly normal (Figure 5a,b,f,g). Nevertheless, cell counts in such apparently normal areas at 11 weeks OVA showed a highly significant 20% decrease in mean density of OSNs plus globose basal cells in OVA-treated versus untreated mice (134.7 ± 4.0 and 169.4 ± 4.1 cells/100 μm, respectively; Figure 6d). In contrast, supporting cell density in these areas remained unchanged (21.1 ± 0.4 vs. 21.6 ± 0.5 cells/100 μm). Counts were made at 11 weeks to maximize the possible differences.

Some increased tearing may occur in these grossly normal areas as well (Figure 5g). Although such tearing often occurs in sectioned epithelial material, it seemed more frequent in the chronic AR OE, suggesting possibly weakened intercellular connections.

In addition, however, scattered small areas of much more noticeable OE thinning, reduced cell density, and distinct disruption or loss of normal OE organization also occurred in chronic OVA animals (Figure 5h–k). Such areas were more obvious with 11 weeks than 6 weeks OVA treatment. By 11 weeks, areas of cellular hypertrophy also appeared (Figure 5k). By their location, the swollen cells appear to be OSNs, but further examination is needed to confirm that they do not represent goblet cell metaplasia to the OE or even swollen supporting cell basal processes.

Interestingly, in many animals, OE disruption appeared somewhat greater in more RE-proximal regions (Figure 5l), regardless of nasal cavity location. An extreme example of this is disappearance of the septal organ, a small OE-containing structure situated in the ventral midseptal RE (Figure 5m,n). In all 11-week OVA animals for which examined sections included this region, the septal organ had been replaced by hypertrophied RE, its original location indicated only by the presence of subepithelial Bowman's glands. A proximity effect was also noticed with BrdU labeling (below).

Except for this possible RE proximity effect, no obvious inter- or intra-animal uniformity occurred in either the degree or nasal distribution of this more pronounced OE

disruption. Rather, histological changes occurred on an individual nasal cavity basis, likely reflecting individual infusion specifics.

Nasal exudate. Despite fixation by transcardial perfusion, noticeable cellular exudate occurred in nasal cavities of several chronic OVA-treated mice (e.g., Figures 3b,d, 5a,b, 9h, 10a,b). This was more pronounced at 11 weeks and in animals showing greater epithelial disorganization. Cells could be seen blebbing from both OE and RE (Figures 5c,d, 10b).

Changes in the OE-associated lamina propria. In contrast to the somewhat limited and variable histological changes in the OE itself, the OE-associated subepithelial Bowman's glands showed pronounced swelling throughout the nasal cavity in chronic OVA animals, apparent in both H&E and Alcian blue preparations (Figures 5f,g and 7). This was greater with 11 than 6 weeks exposure. Swollen acinar regions appeared to both severely crowd neighboring olfactory nerve bundles and to encroach disruptively into the OE (Figures 5f,g,m,n and 7i). Alcian blue staining revealed some slight swelling in chronic PBS animals as well (Figure 7e,f), but no impingement on olfactory nerve bundles or OE. Swelling was minimal with acute PBS or OVA exposure. Possible AR-related Bowman's gland swelling has been previously noted (Getchell and Mellert 1991) but only recently documented (Ozaki et al. 2010), although in the latter report Bowman's glands were not specifically identified as such.

Olfactory nerve bundles also showed reduced axonal packing in chronic OVA mice compared with the other treatment groups, especially at 11weeks exposure (cf. Figure 5f,g with Figure 4b).

Cellular dynamics

Because of the significant RE thickening and the reduced OE cell densities in chronic OVA animals, as well as the well-known changes in OE cellular dynamics following various experimental manipulations (e.g., Graziadei and Monti Graziadei 1978, 1980; Costanzo and Graziadei 1983; Costanzo 1984; Farbman et al. 1988; Carr and Farbman 1992, 1993; Schwob et al. 1992), OE and RE proliferative and degenerative activities were examined in all Series II animals.

Proliferative activity

Untreated animals showed few or no BrdU-labeled cells, and those few were predominantly located in the OE basal cell layer, as expected (Moulton et al. 1970; Graziadei 1973; Graziadei and Monti Graziadei 1978) (Figure 8a,d). The same was true for OVA-acutely exposed and all PBS animals. Thus, neither PBS infusion alone nor acute OVA exposure affects OE or RE proliferative activity.

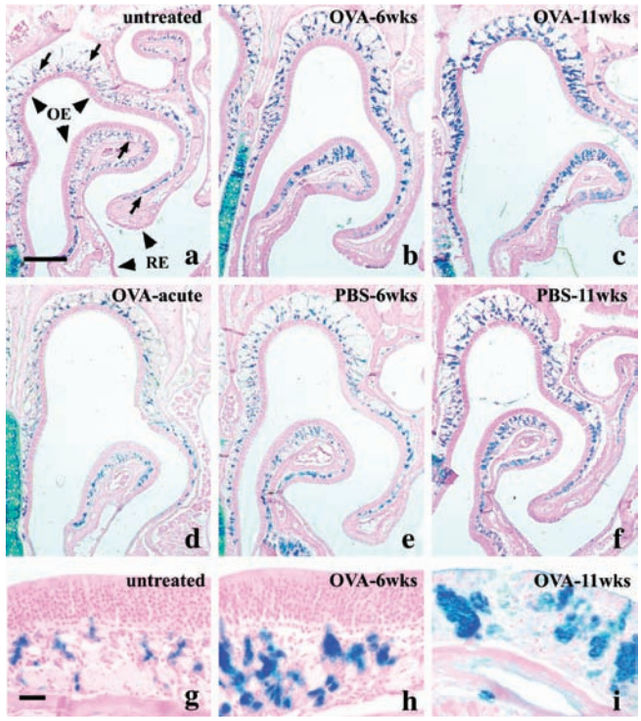

Figure 7 Alcian blue-stained sections showing the relative degree of Bowman's gland swelling with the various treatment regimens. (**a**–**f**) Swelling of the darkly stained Bowman's gland acinar cells (e.g., arrows in a) in the sub-OE *lamina propria* is pronounced in chronic OVA exposure (b, c) but much less with chronic PBS exposure (e, f). None occurs with acute exposure (d). Bowman's glands are absent from the sub-RE *lamina propria* (RE indicated in a). Septal cartilaginous staining also occurs (lower left, a–e). (**g**–**i**) Higher magnifications of OE from untreated and chronically OVA-exposed animals show the distinct swelling in the *lamina propria* at 6 weeks and swelling into the OE itself at 11 weeks. In the latter image, the OE shows extreme disruption and disruption of OE/*lamina propria* boundaries. Image contrast and brightness have been adjusted over the entire figure. Calibration bars, a (for a–f), 250 μm; g (for g–i), 25 μm.

In contrast, chronic OVA exposure caused noticeable BrdU labeling (Figure 8b,c). This occurred primarily in the RE, particularly in strips of contiguous cells with either apically or basally situated nuclei (Figure 8f,g). Goblet cell labeling predominated, but ciliated and some basal cell labeling also occurred, in agreement with the RE cell counts. The large amount of goblet cell labeling reflects goblet cell hyperplasia and likely metaplasia (Rogers 2003; Locksley 2010), which would contribute to both RE swelling and increased mucus production. Absence of RE labeling in all other groups indicates that their slight RE swelling reflects cellular hypertrophy alone rather than hyperplasia.

In the OE, BrdU labeling remained primarily in scattered single basal cells in all treatment groups, (Figure 8b–e). However, chronic OVA mice also showed localized OE regions with apical and/or basal strips of contiguously labeled cells, similar to that in RE, especially in RE-adjacent areas and areas of normally thin OE, such as the concave lateral turbinate surfaces (Figure 8b,c,h–j). In animals showing

greater epithelial disruption, the BrdU-labeled cell strips were more numerous and widespread, including in areas of normally thicker OE that had thinned (Figure 8k). Strips were generally longer and more widespread at 11 weeks OVAs than at 6 weeks OVA (cf. Figure 8b,c,j). Strip length also appeared greater in animals with higher RE-associated eosinophil levels and OVA-specific IgE titers.

The identity of labeled cells in the OE strips was not always clear, a fact worsened by cellular swelling. In some areas, cell identity was apparent from cell location, as with strips of labeled supporting or basal cells (Figure 8h,i), although many of the apparent supporting cells showed abnormally apically situated nuclei with a smaller supranuclear cytoplasmic region than normal. In other areas, however, especially those with more damage, cell identity was uncertain (Figure 8f–i,k,l). Cell-specific markers are needed to address this issue.

Interestingly, in contrast to the scattered single BrdU-labeled basal cells (above), in which nuclear labeling was sharply defined (Figure 8d,e), labeling in all BrdU-labeled cell strips was diffuse and somewhat faint (Figure 8f–i). This likely reflects nuclear swelling and consequent label dispersal within the swollen nuclei: similarly increased intranuclear dispersal and reduced staining intensity in the swollen nuclei occurred using the Feulgen stain, a DNA label (not shown). Labeled cells do not appear necrotic: the diffuse BrdU label always appeared membrane-bound at high magnification. No obvious macrophage infiltration into these areas was observed either. Ultrastructural examination is needed.

Bowman's glands showed no BrdU labeling (Figure 8h,k), indicating that their pronounced swelling reflects acinar cell hypertrophy alone.

Few BrdU-labeled cells were seen in the nasal exudate (Figure 8l).

Degenerative activity

TUNEL labeling patterns (Figure 9) differed noticeably from those of BrdU. First, although only the expected minimal labeling occurred in untreated controls (Figure 9a), TUNEL labeling was seen in all other treatment groups (Figure 9b–h). Such labeling in PBS and acute OVA animals, in clear absence of eosinophil infiltration or elevated IgE titers, indicates that not all TUNEL labeling reflects an AR response. Some must result from fluid infusion alone, with AR-related responses superimposed on that.

TUNEL effects of fluid infusion with AR effects superimposed help explain several other observations, especially when considered in conjunction with the nasal patency cycle (Bojsen-Møller and Fahrenkrug 1971). First, TUNEL labeling in PBS and acute OVA animals tended to be more unilateral than in chronic OVA animals (Figure 9b–g). Second, overall labeling levels with both PBS and OVA were generally higher in the chronically than acutely treated animals (Figure 9b–g). Third, although noticeable interanimal variability occurred in all treatment groups, the degree

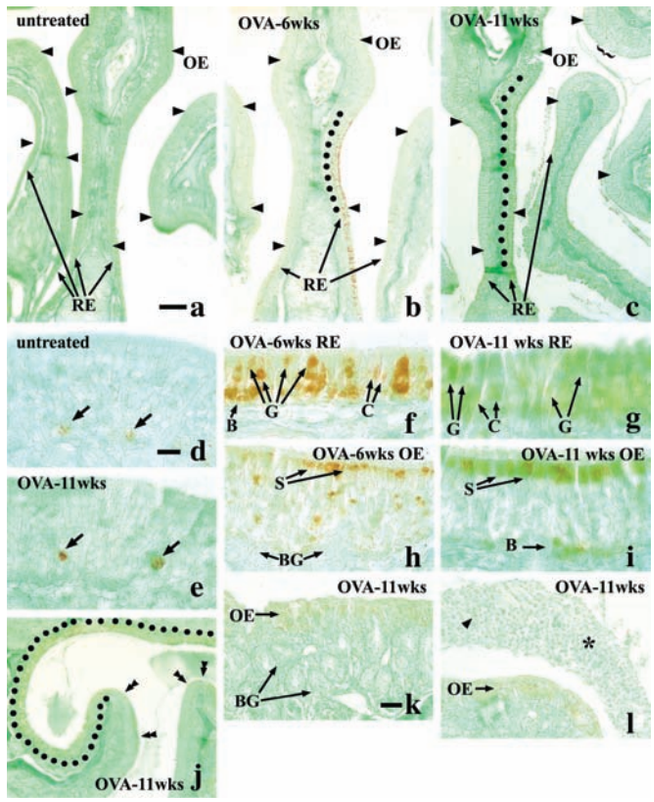

Figure 8 Fast Green-counterstained immunoperoxidase preparations showing BrdU labeling in untreated and chronically OVA-treated animals. (**a**–**c**) Low magnification nasal cavity images showing the dorsal limits of RE (arrows) and the distribution of OE elsewhere (arrowheads). Untreated animals (a), as well as PBS- and acutely OVA-treated animals (not shown), show no labeling except in scattered OE basal cells, better seen at higher magnification (**d**). In contrast, following chronic OVA exposure, strips of contiguous cell labeling occur in much of the RE (b, c). This can be faint, especially in 11-week OVA animals (c, **g**), but is indeed present. (**f**, g) Higher magnification shows that in the RE strips, labeled cells are primarily goblet cells (G) but also include ciliated cells (C) and a few basal cells (B). In most of the OE, labeling remains primarily in scattered basal cells (bracketed turbinate area, upper right, c; **e**, bracketed region of c rotated and at higher magnification), as in untreated animals. However, especially in RE-adjacent areas, strips of OE labeling also occur (subepithelial dots just dorsal to septal RE, b, c). These strips are generally longer in 11-week OVA than 6-week OVA animals. Labeled cells in the OE strips are primarily supporting (S) and basal (B) cells but can also include scattered cells in the intervening olfactory sensory cell layer. The 11-week OVA animals also show wider nasal distribution of labeled cell strips than 6-week animals (**j**). These occurred in normally thinner OE (j, dots, here around the concave surface of endoturbinate 1, left, and the lateral dorsal recess, top) as well as some scattered in normally thicker OE (j, double arrowheads). Labeling also appeared in areas showing greater OE disruption (**k**, **l**). In both RE and OE labeled cell strips, the labeled nuclei are generally quite swollen, more so at 11 weeks OVA than 6 weeks OVA, leading to greater dispersal of immunoreactivity product through increased nuclear volumes and consequently fainter staining (c, g, **i**–l). This contrasts with nuclei of the scattered single labeled basal cells, which remain unswollen and sharply delineated (d, e). (**h**, k) Swollen Bowman's glands (BG) showed no BrdU labeling, even subjacent to disrupted OE-containing labeled cells. (l) Few labeled cells (arrowhead) occur in nasal exudate (asterisk). Image brightness of a, c and contrast of j were increased slightly to better show label distribution. Calibration bars, a, 100 μm for a–c, j; d, 10 μm, for d–i; k, 25 μm for k–l.

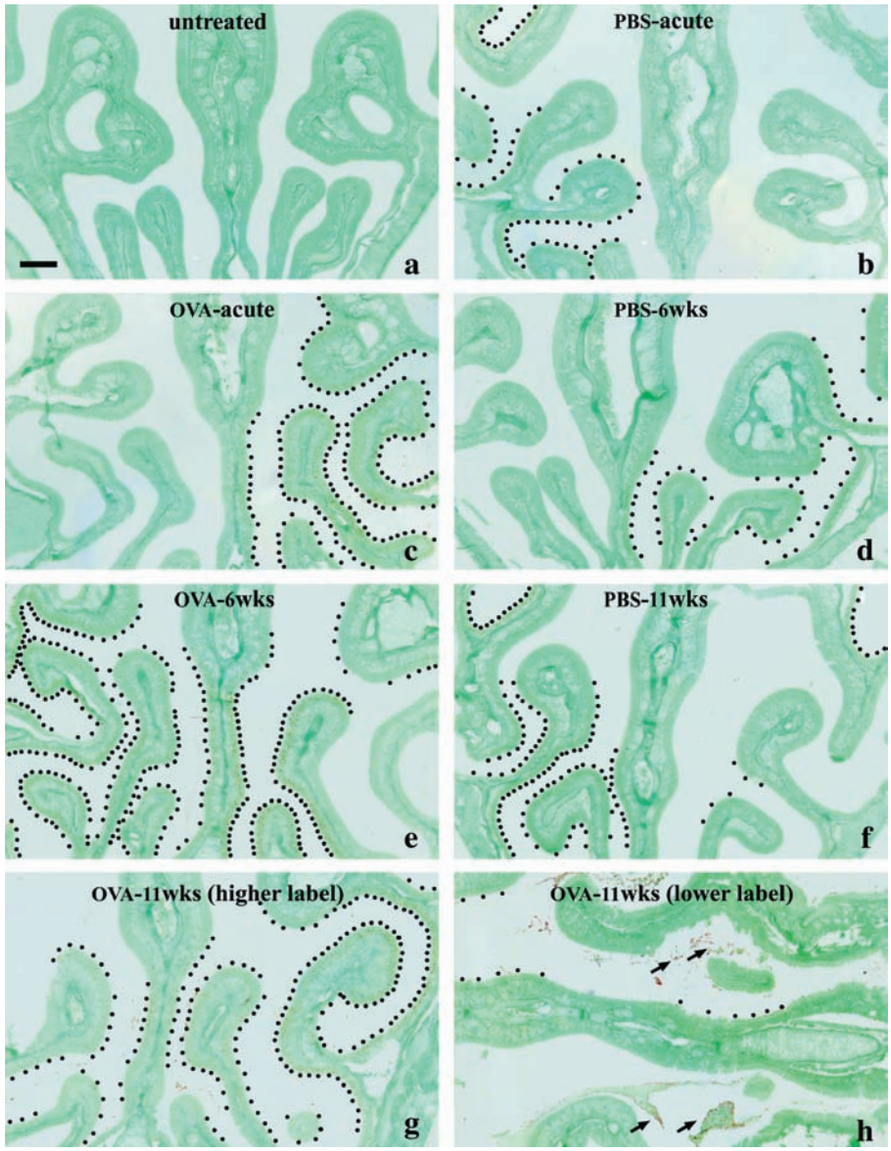

Figure 9 Low magnification images showing TUNEL labeling distributions in nasal cavities in animals receiving different exposure regimens. Dots have been added to indicate the location of labeling, seen at higher magnification of the individual images. Dot densities reflect subjective estimates of the labeling densities. Dorsal is up except in **h**, which has been rotated counterclockwise to show a greater portion of the septum. Untreated animals showed little or no labeling (a). In acutely exposed or chronically PBS-treated animals, labeling is predominantly unilateral (b-d, f). In contrast, 6-week and more highly labeled 11-week OVA animals show bilateral labeling (e, g). Additionally, however, some 11-week OVA animals show high (g) OE labeling levels, whereas others show low levels (h). The latter often show noticeable TUNEL labeling of sloughed cells in nasal cavity exudate in (arrows, h). Brightness of all images was uniformly increased to enhance labeling visibility. Calibration bar, 200 μm.

of variability was generally higher in acutely treated than in chronically treated animals (not shown). Thus, if cyclic alteration in naris patency were sufficient to limit fluid access into the less opened nasal cavity, then acutely treated animals would show lower TUNEL labeling on the less patent side despite delivery of equal fluid volumes to each naris. In contrast, the multiple infusions of chronic treatment would, over the entire experimental time course, lead to cumulative effects in both nasal cavities, resulting in the higher overall labeling levels and lower labeling variability in chronic than in acute animals. With chronic PBS treatment, however, those cumulative effects would reflect only general epithelial damage, not an AR response. If the greatest damage present at the time of sacrifice were due to the most recent PBS delivery, this would still reflect the nasal patency at the time of that final infusion, but now imposed on labeling effects of cumulative damage. In contrast, the chronic OVA multiple infusions would lead to cumulative effects of immune responses in both nasal cavities, evidenced by bilateral eosinophilic infiltration, and to consequently bilateral TUNEL labeling.

Overall TUNEL nasal distribution in both PBS- and OVA-chronically treated animals was generally more extensive at

11 than 6 weeks (Figure 9f,g vs. d,e), again likely reflecting greater cumulative effects with longer treatment. However, although some of the 11-week OVA mice showed clearly increased TUNEL labeling relative to chronic PBS mice (Figure 9g), others showed distinctly less (Figure 9h). Significantly, the OVA-treated animals with lower labeling also showed the most pronounced OE disruption and cell sloughing, with many sloughed cells being TUNEL positive (arrows, Figures 9h and 10a,b). This suggests that the lower labeling levels in these mice may actually reflect greater and/or more rapid loss of damaged cells.

Finally, in further contrast to BrdU, TUNEL-positive cells were noticeably more numerous in OE than RE (Figure 10c). Specific cell type labeling patterns also differed from BrdU labeling: in the RE, ciliated cells showed greater labeling than goblet or basal cells (Figure 10d); in the OE, most labeling occurred in the OSN layer, although scattered labeling occurred in supporting and basal cell layers as well (Figure 10e). Labeled OE cells showed no swelling.

Nasal sinuses

AR-related changes were also noted in the nasal sinuses, including epithelial hypertrophy, subepithelial eosinophil infiltration, and BrdU and TUNEL labeling (See Figures 4, 5). These are mentioned because sinusitis can similarly lead to olfactory impairment.

Discussion

Our study examined murine nasal epithelial changes following AR induction using the McCusker nasal sensitization and challenge protocol (McCusker et al. 2002). AR induction was indicated by high OVA-specific IgE serum levels and eosinophil infiltration and occurred only in chronically OVA-exposed animals.

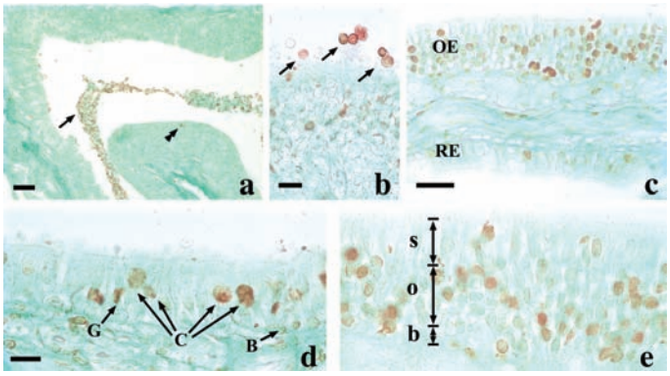

Figure 10 Higher magnifications of nasal TUNEL reactivity in chronically OVA-treated animals (**a**, **b**, 11 weeks; **c**–**e**, 6 weeks treatment). (a) Section from an animal that showed little OE reactivity. Only a single reactive cell is apparent (double arrowhead) in the OE while much labeling occurs in sloughed cells in nasal exudate (arrow). (b) Numerous TUNEL-labeled cells sloughing from OE (e.g., arrows). (c) Section across a turbinate showing the different labeled cell densities in OE and RE. (d) RE section showing higher labeling in ciliated (C) than goblet (G) or basal (B) cells. (e) OE section showing labeling primarily in the OSN layer (o) and less labeling in supporting (s) and basal (b) cell layers. Calibration bars, a, 50 μm; b, 10 μm; c, 25 μm; d, 10 μm, for d, e.

The most striking finding was the localization in chronic OVA animals of eosinophil infiltration to the immediate RE-subjacent, but not OE-subjacent, *lamina propria*. Similar eosinophilic localization has been previously noted and preliminarily investigated in mice by Hussain et al. (2001) using quite different AR sensitization and challenge protocols, but received little further attention. With interest focused on AR per se, Hussain et al. and the few others who subsequently cite them (Hussain et al. 2002; Sasaki et al. 2007; Hayahashi et al. 2008) simply limited investigation to RE-only nasal regions, with minimal examination of localization specificity. Other AR researchers, using various allergens and protocols in a variety of species, have either made no distinction between OE and RE or examined only the RE without further comment (e.g., Tanaka et al. 1988; Takahashi et al. 1990; Ishida et al. 1993; Asakura et al. 1998; van de Rijn et al. 1998; Okano et al. 1999; McCusker et al. 2002; Lin et al. 2010). Much AR literature has also focused on human nasal tissue; and although eosinophil involvement is well known from nasal swab and mucus preparations or biopsies, those sampling methods provide no explicit information on eosinophil tissue localization. Overall, such inadequacies have led to limited awareness or concern about RE/OE eosinophil localization specificity in AR.

A few reports of eosinophil infiltration of OE-associated tissue do exist, but those raise other issues. Using OVA as the allergen, Ozaki et al. (2010) reported significant infiltration of OE *lamina propria* by eosinophils and other inflammatory cell types. However, lack of clarity as to OE versus RE identity and nasal distribution were apparent in that report. Moreover, a very different immunization protocol from our own was followed, including use of 2000 times the OVA infusion amount that could lead to other, non-AR responses (McCusker et al. 2002). Finally, in our own laboratory, Epstein et al. (2008) found OE eosinophil infiltration following nasal sensitization to *Aspergillis fumigatus* extract. Observed responses, however, included large increases in OE apoptosis 12–18 h after single infusions of extract in absence of previous sensitization. This suggests involvement of additional, nonallergenic responses, such as innate responses to fungal microbe-associated molecular patterns, a concern whenever microbially derived or associated allergens are used.

Although we did not verify the full extent of infusate nasal dispersion, for example, by examining perfused vital dye nasal distribution, the observed eosinophil RE localization does not seem due simply to inadequate OVA access to the OE during infusion. First, RE-associated eosinophil localization occurred uniformly throughout the entire nasal cavity, anteriorly, posteriorly, and laterally and in RE-bearing concave turbinate surfaces. Other, specifically OE-associated changes, such as Bowman's gland swelling and altered OE TUNEL labeling, were also uniformly distributed. Second,

limited OVA nasal distribution would also not explain the uniformly abrupt change in sublaminal eosinophil infiltration seen across all RE/OE transition zones in all chronic OVA animals. Finally, the similar observations of Hussain et al. (2001) occurred with systemic adjuvant-enhanced OVA sensitization and 2 different nasal challenge protocols from our own, one a continuous 20 min exposure to nebulized OVA twice a day 6 days apart, the other a daily intranasal OVA infusion for 10 days. Thus, although without definitive verification we cannot guarantee that OVA solution uniformly reached all parts of the nasal cavity with each individual application, the RE-specific subepithelial eosinophil infiltration does appear real.

The cause for this localization specificity is unknown. In preliminary examination, Hussain et al. (2001) found no differential RE versus OE immunostaining for either I-CAM-1 or eotaxin. Those factors were examined because of their known induction in human AR and possible roles, respectively, in transepithelial eosinophil migration and as an eosinophil cytokine. Within the RE itself, ciliated cells can interact with allergens (Locksley 2010) to initiate local allergic responses (Coffman 2010). Goblet cells can also be involved (Rogers 2003). Thus, subsequently released eosinophil attractants might be localized within RE-associated *lamina propria*. Alternatively, OE mucosa may in some way block sub-OE eosinophil infiltration or OE and RE may provide differential transepithelial allergen access. Absence of OE-associated eosinophil infiltration might protect the OE from inflammatory processes, thereby representing an extension of the immune privilege of various neural tissues. Examination of distribution specificities of other immune cell types, including mast cells, basophils, neutrophils, macrophages, and T_H2 cells, as well as related RE versus OE cytokine and cytokine receptor analysis, are needed.

Also curious was the absence of large-scale OE cell loss (only 20%), thinning, or disruption in the chronic OVA animals except at localized sites, especially given the high levels of OE TUNEL, limited increases in BrdU labeling, and absence of spatial and temporal BrdU and TUNEL overlap. Hussain et al. (2001) also observed relatively little AR-induced OE damage. Given the massive OSN death and replacement following direct OSN surgical and chemical damage (e.g., Graziadei and Monti Graziadei 1978; Carr and Farbman 1992; Schwob et al. 1995), greater general OE cell loss and thinning were expected.

We have no ready explanation for these observations. Some specifically AR-associated OE TUNEL labeling may reflect elimination of metaplastic RE cells from the OE as a means of maintaining OE integrity and maximizing olfactory function under AR conditions. Different mechanisms regulating spatial and temporal correlation of OSN cell death and replacement, such as an increased role for active extrusion of damaged cells, may also be involved in AR. As noted, animals showing the fewest TUNEL-positive OE cells showed the greatest OE disruption and cell sloughing, with many extruded cells being TUNEL positive. Specifically decreased epithelial intercellular adhesion has indeed been reported in bronchial asthma (Trautmann et al. 2005); and specific targeting of degenerating cells for extrusion has been hypothesized to enhance epithelial barrier maintenance in other tissues (Rosenblatt et al. 2001). It may also explain the apparently increased OE tearing in chronic OVA mice.

It is also possible that some TUNEL labeling may reflect false positive labeling (Stähelin et al. 1998; Sloop et al. 1999; Pulkkanen et al. 2000; Walker and Quirke 2001). However, this was carefully monitored. Proteinase K and TdT concentrations were adjusted to minimize background labeling in neighboring tissues and olfactory bulbs. Observed responses were also specific to the epithelia and nasal location, including side-to-side differences in PBS- and acutely OVA-exposed animals and occurrence of only minimal labeling in untreated controls. Finally, sections from previously unilaterally bulbectomized mice (Robinson et al. 2003) processed in parallel with sections from the current study showed appropriately increased TUNEL labeling in ipsilateral OE. Labeling might also reflect necrosis although no macrophage influx or swelling of labeled cells was observed.

Despite the absence of major generalized OE disruption, AR-related OE changes clearly occur. These include localized areas of disruption and major thinning and others of cellular hypertrophy, as well as the Bowman's gland hypertrophy, BrdU and TUNEL labeling, and cell sloughing discussed above. At least some of these changes may be RE-mediated, suggesting the possibility of unexpected RE/OE interactions. One such change is OE BrdU uptake. At 6 weeks of OVA exposure, OE BrdU labeling occurs primarily in more RE-proximal OE and areas of normally thinner OE; by 11weeks exposure, it is more widespread. Most of the thinner OE where labeling occurs lies laterally and on turbinate shafts, where nasal architecture is somewhat complex and might serve to localize any factors released by nearby RE or any RE-associated immune cells. As resulting local OE damage ensues, possible OE replacement by RE (Yee et al. 2009) could increase concentrations of such factors, leading to the increasingly widespread labeling. An extreme example of RE-proximal OE effects may be the disappearance of the RE-surrounded septal organ. Such RE-associated OE effects would also contribute to AR interanimal variability.

Other OE changes may be more locally generated. For example, olfactory nerve compression has been hypothesized to cause retrograde OSN damage in a genetically induced murine rhinosinusitis model (Lane et al. 2010). Swollen Bowman's gland crowding of olfactory nerve bundles and swelling into the OE itself might similarly cause OSN damage in the current study. Certainly, olfactory nerve bundle axonal packing densities are less. Bowman's glands and olfactory nerve ensheathing cells also release immune barrier-associated agents (Getchell ML and Getchell TV 1991; Getchell and

Mellert 1991; Vincent et al. 2005; Débat et al. 2007) that might further affect the OE. Supporting cells, which show a variety of responses to many OE insults (Suzuki et al. 1995, 1996; Carr et al. 2001; Carr 2005; Jia et al. 2009), may also be involved. Supporting cell electrical coupling (Vogalis et al. 2005) might also be related to the apical OE strips of contiguous BrdU cell labeling seen after chronic OVA.

In the RE, TUNEL levels were noticeably low in many AR animals. Interestingly, observations in several species and a variety of inflammatory conditions indicate that airway goblet cell hyperplasia is associated with increased expression of antiapoptotic Bcl-2 (Tesfaigzi et al. 1998, 2000; Harris et al. 2005) and loss of proapoptotic Bim (Pierce et al. 2006), maximizing goblet cell numbers and subsequent mucus secretion. Significantly, with termination of allergen exposure, goblet cell Bcl-2 expression decreases and metaplastic goblet cells disappear from airway mucosae. Analysis of RE TUNEL levels and temporal patterns of any changes following cessation of OVA exposure in AR animals would be of interest.

Our findings also demonstrate that changes were induced by PBS alone, including TUNEL labeling and slight RE swelling with PBS and acute OVA and slight Bowman's gland hypertrophy with chronic PBS. All occurred in absence of eosinophil infiltration, BrdU uptake, or other histological changes. The slight RE and Bowman's gland swelling likely reflect their involvement in increased mucus synthesis, with its protective and olfactory functions (Getchell and Mellert 1991; Rogers 2003; Débat et al. 2007), directed at restoring normal nasal fluid composition after PBS infusion. The TUNEL findings likely reflect fluid infusion-related tissue stress, as described. Whether these reflect specific PBS tonicity, composition, or pH effects or purely mechanical effects of fluid infusion is unclear.

Finally, the amount of any olfactory functional loss in the current model is unknown and needs to be addressed, using both olfactory bulb activity markers and behavioral studies. The lack of major histological OE changes, the significant goblet cell hypertrophy and hyperplasia, and obvious presence of nasal mucus in the 11-week OVA animals, however, suggest that any effects would likely be due predominantly to diminished odorant access to the OE, that is, conductive rather than sensorineural in nature (Snow 1991). This is supported by findings in the Ozaki et al. (2010) study, showing impaired olfactory function and lower olfactory bulb tyrosine hydroxylase immunostaining despite only minor OE histological changes and no change in bulb OMP immunostaining. Sensorineural effects, however, might also be involved, depending on the degrees of OSN damage from Bowman's gland olfactory nerve bundle compression, of increasing OE damage with increased OVA exposure time, and of any neuroma formation. The last was seen in both Series I 11-week OVA mice (not shown).

In conclusion, our study has demonstrated tissue-specific OE and RE effects of AR. It also leaves many questions unanswered: the array of immune cells involved, their specific nasal localizations, and epithelial-specific effects of agents released by each; chemokine and cytokine receptor distributions; different allergens and allergen dosage effects; degree of goblet cell OE metaplasia; recovery time after cessation of chronic allergen exposure; identity and roles of constituent OE cells involved; analysis of OSN cell death versus replacement; and analysis of induced AR on olfactory capability. Species and strain specificities also need further study. Addressing these questions will help clarify the immune system, RE, and OE interactions involved.

Funding

This research was funded by the Department of Otolaryngology—Head and Neck Surgery, Northwestern University from in-house funds.

Acknowledgements

The authors express appreciation to Drs Christine McCusker, Robert Schleimer, and Karen Yee for helpful advice and comments.

References

Apter AJ, Mott AE, Frank ME, Cline JM. 1995. Allergic rhinitis and olfactory loss. Ann Allergy Asthma Immunol. 75:311–316.

Asakura K, Saito H, Watanabe M, Ogasawara H, Matsui T, Kataura A. 1998. Effects of anti-IL-5 monoclonal antibody on the murine model of nasal allergy. Internat J Allergy Immunol. 116:49–52.

Baroody FM, Naclerio RM. 1991. Allergic rhinitis. In: Getchell TV, Doty RL, Bartoshuk LM, Snow JB, editors. Smell and taste in health and disease. New York: Raven Press. p. 529–552.

Bojsen-Møller F, Fahrenkrug J. 1971. Nasal swell-bodies and cyclic changed in the air passage of the rat and rabbit nose. J Anat. 110:25–37.

Carr VMcM. 2005. Induced and constitutive heat shock protein expression in the olfactory system—a review, new findings, and some perspectives. J Neurocytol. 34:269–293.

Carr VMcM, Farbman AI. 1992. Ablation of the olfactory bulb up-regulates the rate of neurogenesis and induces precocious cell death in olfactory epithelium. Exp Neurol. 115:55–59.

Carr VMcM, Farbman AI. 1993. The dynamics of cell death in the olfactory epithelium. Exp Neurol. 124:308–314.

Carr VMcM, Menco BPhM, Yankova MP, Morimoto RI, Farbman AI. 2001. Odorants as cell-type specific activators of a heat shock response in the rat olfactory mucosa. J Comp Neurol. 432:425–439.

Coffman RL. 2010. The origin of T_H2 responses. Science. 328:1116–1117.

Costanzo RM. 1984. Comparison of neurogenesis and cell replacement in the hamster olfactory system with and without a target (olfactory bulb). Brain Res. 307:295–301.

Costanzo RM, Graziadei PPC. 1983. A quantitative analysis of changes in the olfactory epithelium following bulbectomy in the hamster. J Comp Neurol. 215:370–381.

Débat H, Eloit C, Blon F, Sarazin B, Henry C, Huet J-C, Trottier D, Pernollet J-C. 2007. Identification of human olfactory cleft mucus proteins using proteomic analysis. J Proteome Res. 6:1985–1996.

Epstein VA, Bryce PJ, Conley DB, Kern RC, Robinson AM. 2008. Intranasal *Aspergillus fumigatus* exposure induces eosinophilic inflammation and olfactory sensory neuron cell death in mice. Otolaryngol Head Neck Surg. 138:334–339.

Farbman AI, Brunjes PC, Rentfro L, Michas J, Ritz S. 1988. The effect of unilateral naris occlusion on cell dynamics in the developing rat olfactory epithelium. J Neurosci. 8:3290–3295.

Getchell ML, Getchell TV. 1991. Immunohistochemical localization of components of the immune barrier in the olfactory mucosae of salamanders and rats. Anat Rec. 231:358–374.

Getchell ML, Mellert TK. 1991. Olfactory mucus secretion. In: Getchell TV, Doty RL, Bartoshuk LM, Snow JB, editors. Smell and taste in health and disease. New York: Raven Press. p. 83–95.

Graziadei PPC. 1973. Cell dynamics in the olfactory mucosa. Tissue Cell. 5:113–115.

Graziadei PPC, Monti Graziadei GA. 1978. Continuous nerve cell renewal in the olfactory system. In: Jacobson M, editor. Handbook of sensory physiology, vol. IX. Development of sensory systems. Berlin (Germany): Springer-Verlag. p. 55–82.

Graziadei PPC, Monti Graziadei GA. 1980. Neurogenesis and neuron regeneration in the olfactory epithelium of mammals. III. Deafferentation and reinnervation of the olfactory bulb following section of the filia olfactoria in rat. J Neurocytol. 9:145–162.

Harris JF, Fischer MJ, Hotchkiss JR, Monia BR, Randell SH, Harkema JR, Tesfaigzi Y. 2005. Bcl-2 sustains increased mucous and epithelial cell numbers in metaplastic airway epithelium. Am J Respir Crit Care Med. 171:764–772.

Hussain I, Randolph D, Brody SL, Song S-K, Hsu A, Kahn AM, Chaplin DD, Hamilos DL. 2001. Induction, distribution and modulation of upper airway allergic inflammation in mice. Clin Exp Allergy. 31:1048–1059.

Hussain I, Jain VV, Kitagaki K, Businga TR, O'Shaughnessy P, Klein JN. 2002. Modulation of murine allergic rhinosinusitis by CpG oligodeoxynucleotides. Laryngoscope. 112:1819–1826.

Hayahashi T, Hasegawa K, Sasaki Y. 2008. Systemic administration of olygodeoxynucleotides with CpG motifs at priming phase reduces local Th2 response and late allergic rhinitis in BALB/c mice. Inflammation. 31:47–55.

Ishida M, Amesara R, Ukai K, Sakakura Y. 1993. Antigen (DPN-As)-induced allergic rhinitis model in guinea pigs. Ann Allergy. 72:240–244.

Jia C, Doherty JP, Crudgington S, Hegg CC. 2009. Activation of purinergic receptors induces proliferation and neuronal differentiation in Swiss Webster mouse olfactory epithelium. Neuroscience. 163:120–128.

Lane AP, Turner J, May L, Reed R. 2010. A genetic model of chronic rhinosinusitis-associated olfactory inflamation reveals reversible functional impairment and dramatic neuroepithelial reorganization. J Neurosci. 30:2324–2329.

Liebeck HG. 1975. Zum Bau der oberen Luftwege der weissen Ratte (*Mus rattus norvegicus*, var., *albinos*). Anat Anz. 138:170–179.

Lin L, Zheng CQ, Zhang LP, Da CD, Zhao KQ. 2010. Up-regulation of of Orai 1 in murine allergic rhinitis. Histochem Cytochem. 134:93–102.

Locksley RM. 2010. Asthma and allergic inflammation. Cell. 140:777–783.

Luna LG. 1968. Manual of histologic staining methods of the armed forces institute of pathology. 3rd ed.. New York: McGraw-Hill. p. 111–112.

Martin P, Villares R, Rodriguez-Mascarenhas S, Zaballos A, Leitges M, Kovac J, Sizing I, Rennert P, Marquez G, Marinez-A C, et al. 2005. Control of T helper 2 cell function and allergic airway inflammation by PKCζ. Proc Natl Acad Sci U S A. 102:9866–9871.

McCusker C, Chicoine M, Hamid Q, Mazer B. 2002. Site-specific sensitization in a murine model of allergic rhinitis: role of the upper airway in lower airways disease. J Allergy Clin Immunol. 110:891–898.

Moulton DG, Celebi G, Fink RP. 1970. Olfaction in mammals–two aspects: proliferation of cells in the olfactory epithelium and sensitivity to odours. In: Wolstenholme GEW, Knight J, editors. Ciba foundation symposium on taste and smell in vertebrates. London: Churchill Press. p. 227–250.

Okano M, Nishizaki K, Abe M, Wang M-M, Yoshino T, Satoskar AR, Masuda Y, Harn DA Jr. 1999. Strain-dependent induction of allergic rhinitis without adjuvant in mice. Allergy. 54:593–601.

Ozaki S, Toida K, Suzuki M, Nakamura Y, Ohno N, Ohasi T, Nakayama M, Hamajima Y, Inagaki A, Kitaoka K, et al. 2010. Impaired olfactory function in mice with allergic rhinitis. Auris Nasus Larynx. 37:575–583.

Pierce J, Rir-Sima-Ah J, Estrada I, Wilder J, Strasser A, Tesfaigzi Y. 2006. Loss of pro-apoptotic Bim promotes accumulation of pulmonary T lymphocytes and enhances allerfen-induced goblet cell metaplasia. Am J Physiol Lung Cell Mol Physiol. 291:L862–L870.

Pulkkanen KJ, Laukkanen MO, Naarala J, Yla-Herttuaia S. 2000. False-positive apoptosis signal in mouse kidney and liver detected with TUNEL assay. Apoptosis. 5:329–333.

Rahman A, Yatsuzuka R, Jiang S, Ueda Y, Kamei C. 2006. Involvement of cyclooxogenase-2 in allergic inflammation in rats. Internat Immunopharmacol. 6:1736–1742.

Robinson AM, Conley DB, Kern RC. 2003. Olfactory neurons in bax knockout mice are protected from bulbectomy-induced apoptosis. Neuroreport. 14:1891–1894.

Rogers DF. 2003. The airway goblet cell. Int J Biochem Cell Biol. 35:1–6.

Rosenblatt J, Raff MC, Cramer LP. 2001. An epithelial cell destined for apoptosis signals its neighbors to extrude it by an actin- and myosin-dependent mechanism. Curr Biol. 11:1847–1857.

Saito H, Howie K, Waattie J, Denberg A, Ellis R, Inman MD, Denberg JA. 2001. Allergen-induced murine upper airway inflammation: local and systemic changes in murine experimental allergic rhinitis. Immunology. 104: 226–234.

Sasaki Y, Hayashi T, Hasegawa K. 2007. Lactate dehydrogenase-elevating virus infection at the sensitization and challenge phases reduces the development of delayed eosinophilic allergic rhinitis in BALB/c mice. Scand J Immunol. 66:628–635.

Sato J, Asakura K, Murakami M, Uede T, Kaaura A. 1999. Topical CTLA4-Ig suppresses ongoing mucosal immune responses in presensitized murine model of allergic rhinitis. Int Arch Allergy Immunol. 119:197–204.

Schwob JE, Szumowski KEM, Stasky AA. 1992. Olfactory sensory neurons are trophically dependent on the olfactory bulb for their prolonged survival. J Neurosci. 12:3896–3919.

Schwob JE, Youngentob SL, Mezza RC. 1995. Reconstitution of the rate olfactory epithelium after methyl bromide-induced lesion. J Comp Neurol. 359:15–37.

Sloop GD, Roa JC, Delgado AG, Balart JT, Hines MO III, Hill JM. 1999. Histological sectioning produces TUNEL reactivity. A potential cause of false-positive staining. Arch Pathol Lab Med. 123:529–532.

Snow JB. 1991. Causes of olfactory and gustatory disorders. In: Getchell TV, Doty RL, Bartoshuk LM, Snow JB, editors. Smell and taste in health and disease. New York: Raven Press. p. 445–449.

Stähelin BJ, Marti U, Soloioz M, Zimmerman H, Reichen J. 1998. False positive staining in the TUNEL assay to detect apoptosis in liver and intestine is caused by endogenous nucleases and inhibited by diethyl pyrocarbonate. J Clin Pathol Mol Pathol. 51:204–208.

Suzuki Y, Shafer J, Farbman AI. 1995. Phagocytic cells in the rat olfactory epithelium after bulbectomy. Exp Neurol. 136:225–233.

Suzuki Y, Takeda M, Farbman AI. 1996. Supporting cells as phagocytes in the olfactory epithelium after bulbectomy. J Comp Neurol. 376:509–517.

Takahashi N, Aramaki Y, Tsuchiya S. 1990. Allergic rhinitis model with brown Norway rat and evaluation of antiallergic drugs. J Pharmacobiol Dynam. 13:414–420.

Tanaka K-I, Okamoto Y, Nagaya Y, Nishimura F, Takeoka A, Hanada S, Kohno S, Kawai M. 1988. A nasal allergy model developed in the guinea pig by intranasl application of 2,4-toluene diisocyanate. Internat Arch Allergy Appl Immunol. 85:392–397.

Tesfaigzi J, Hotchkiss JA, Harkema JR. 1998. Expression of the Bcl-2 protein in nasal epithelia of F344/N rats during mucous cell metaplasia and remodeling. Am J Respir Cell Mol Biol. 18:794–799.

Tesfaigzi Y, Fischer MJ, Martin MJ, Seagrave J. 2000. Bcl-2 in LPS- and allergen-induced hyperplastic mucous cells in airway epithelia of Brown Norway rats. Am J Physiol Lung Cell Mol Physiol. 279:L1210–L1217.

Trautmann A, Krüger K, Akdis M, Müller-Wening Akkaya A, Bröker E-B, Blaser K, Akdis CA. 2005. Apoptosis and loss of adhesion of bronchial epithelial cells in asthma. Int Arch Allergy Immunol. 138:142–150.

van de Rijn M, Mehlhop PD, Judkins A, Rothenberg ME, Luster AD, Oettgen HC. 1998. A murine model of allergic rhinitis: studies on the role of IgE in the pathogenesis and analysis of the eosinophil influx elicited by allergen and eotaxin. J Allergy Clin Immunol. 74:65–74.

Vincent AJ, West AK, Chuah MI. 2005. Morphological and functional plasticity of olfactory ensheathing cells. J Neurocytol. 34:65–80.

Vogalis F, Hegg CC, Lucero MT. 2005. Electrical coupling in sustentacular cells of the mouse olfactory epithelium. J Neurophysiol. 94:1001–1012.

Walker JA, Quirke P. 2001. Viewing apoptosis through a 'TUNEL'. J Pathol. 195:275–276.

Yee KK, Pribitkin EA, Cowart BJ, Rosen D, Feng P, Rawson NE. 2009. Analysis of the olfactory mucosa in chronic rhinosinusitis. Ann NY Acad Sci. 1170:590–595.